What Causes the Divergences in Local Second-Order Closure Models?

V. M. CANUTO

NASA Goddard Institute for Space Studies, New York, and Department of Applied Physics and Mathematics, Columbia University, New York, New York

Y. CHENG

NASA Goddard Institute for Space Studies, New York, New York

A. M. HOWARD

NASA Goddard Institute for Space Studies, New York, New York, and Department of Earth, Atmospheric and Planetary Sciences, Massachusetts Institute of Technology, Cambridge, Massachusetts

(Manuscript received 17 March 2004, in final form 10 September 2004)

ABSTRACT

It has been known for three decades that in the case of buoyancy-driven flows the widely used second-order closure (SOC) level-2.5 turbulence models exhibit divergences that render them unphysical in certain domains. This occurs when the dimensionless temperature gradient G_h (defined below) approaches a critical value G_h(cr) of the order of 10; thus far, the divergences have been treated with ad hoc limitations of the type

$$G_h \le G_h(\mathrm{cr}) \sim 10, \quad G_h \equiv -\tau^2 g\alpha \frac{\partial T}{\partial z},$$

where τ is the eddy turnover time scale, g is the gravitational acceleration, α is the coefficient of thermal expansion, T is the mean potential temperature, and z is the height. It must be noted that large eddy simulation (LES) data show no such limitation. The divergent results have the following implications. In most of the $\partial T/\partial z < 0$ portion of a convective planetary boundary layer (PBL), a variety of data show that τ increases with z, $-\partial T/\partial z$ decreases with z, and G_h decreases with z. As one approaches the surface layer from above, at some z_{cr} ($\sim 0.2H$, H is the PBL height), G_h approaches G_h(cr) and the model results diverge. Below z_{cr}, existing models assume the displayed equation above. Physically, this amounts to artificially making the eddy lifetime shorter than what it really is. Since short-lived eddies are small eddies, one is essentially changing large eddies into small eddies. Since large eddies are the main contributors to bulk properties such as heat, momentum flux, etc., the artificial transformation of large eddies into small eddies is equivalent to *underestimating the efficiency of turbulence as a mixing process.*

In this paper the physical origin of the divergences is investigated. First, it is shown that it is due to the local nature of the level-2.5 models. Second, it is shown that *once an appropriate nonlocal model is employed, all the divergences cancel out, yielding a finite result.* An immediate implication of this result is the need for a reliable model for the third-order moments (TOMs) that represent nonlocality. The TOMs must not only compare well with LES data, but in addition, they must yield nondivergent second-order moments.

1. Second-order closure model equations

For simplicity, we study a purely convective planetary boundary layer (PBL). The governing equations for the second moments are [see Mellor and Yamada (1974, 1982, hereafter MY74 and MY82, respectively); Eqs. (A16)–(A45) in Canuto (1994); Cheng et al. (2002, hereafter CCH), their Eqs. (2a)–(4b)]:

$$\frac{\partial}{\partial t}\left(\overline{w^2} - \frac{1}{3}\overline{q^2}\right) = -\frac{\partial F_w}{\partial z} - \frac{5}{\tau}\left(\overline{w^2} - \frac{1}{3}\overline{q^2}\right) + \frac{20}{3}\lambda_4 g\alpha\overline{w\theta}, \tag{1a}$$

$$\frac{\partial}{\partial t}\left(\overline{u^2} - \frac{1}{3}\overline{q^2}\right) = \frac{1}{2}\frac{\partial F_w}{\partial z} - \frac{5}{\tau}\left(\overline{u^2} - \frac{1}{3}\overline{q^2}\right) - \frac{10}{3}\lambda_4 g\alpha\overline{w\theta}, \tag{1b}$$

$$\frac{\partial}{\partial t}\overline{w\theta} = -\frac{\partial}{\partial z}\overline{w^2\theta} - \lambda_5\frac{\overline{w\theta}}{\tau} - \overline{w^2}\frac{\partial T}{\partial z} + \lambda_0 g\alpha\overline{\theta^2}, \tag{1c}$$

Corresponding author address: Dr. V. M. Canuto, NASA Goddard Institute for Space Studies, 2880 Broadway, New York, NY 10025.
E-mail: vcanuto@giss.nasa.gov

$$\frac{\partial}{\partial t}\overline{\theta^2} = -\frac{\partial}{\partial z}\overline{w\theta^2} - 2\frac{\lambda_0}{\lambda_8}\frac{\overline{\theta^2}}{\tau} - 2\overline{w\theta}\frac{\partial T}{\partial z}, \quad (1d)$$

$$\frac{\partial}{\partial t}K = -\frac{1}{2}\frac{\partial}{\partial z}(\overline{q^2w} + 2\overline{pw}) + g\alpha\overline{w\theta} - \frac{2K}{\tau}, \quad (1e)$$

where

$$F_w \equiv \overline{w^3} - \frac{1}{3}\overline{q^2w} + \frac{4}{3}\overline{pw}, \quad (1f)$$

$$q^2 \equiv w^2 + 2u^2, \quad 2K = \overline{q^2}. \quad (1g)$$

In Eqs. (1a)–(1e) the dependent variables are the vertical and horizontal components $\overline{w^2}$ and $\overline{u^2}$ of twice the turbulent kinetic energy K, the heat flux $\overline{w\theta}$, the turbulent temperature variance $\overline{\theta^2}$, and K; τ is the eddy turnover time scale, g is the gravitational acceleration, α is the coefficient of thermal expansion, T is the mean potential temperature, p is the pressure fluctuation, and z is the height; the λs are the model constants following CCH. The terms F_w, $\overline{w^2\theta}$, and $\overline{w\theta^2}$ are the third-order moments (TOMs) that will be discussed below.

2. Third-order moments

Until 1994, all models for the TOMs were heuristic and most of them used the so-called downgradient approximation (DGA). Canuto et al. (1994) were the first to analytically solve the dynamic equations for the TOMs under the quasi-normal approximation (QNA) for the fourth-order moments. The resulting TOMs exhibited new and unexpected features. 1) Every TOM turned out to be given by the sum of the gradients of all second-order moments rather than by the gradient of only one of them, as assumed in the DGA; 2) the model TOMs compared favorably with LES data; and 3) the model TOMs when used in a full simulation of a convectively driven PBL compared satisfactorily with available data. For further studies on this topic, see Zilitinkevich et al. (1999, their section 3) and Canuto et al. (2001a,b, their sections 3).

3. The divergence problem in the local approximation

Studies of turbulence flows can seldom afford to employ the full set of time-dependent, diffusive Reynolds stress model (RSM) equations, (1a)–(1e) and, furthermore, the initial/boundary conditions needed to solve these differential equations may be difficult to obtain. MY74 and MY82 called the full model the level-4 model; the level-3 models employ only two differential equations, those for K and $\overline{\theta^2}$ (kinetic and potential energies); level-2.5 models retain only the differential equation for K; in level-2 models, all the differential equations reduce to algebraic relations.

In the last 30 years, level-2.5 models have been the most widely used in geophysical studies of turbulent mixing in the atmosphere and the ocean. These models have, however, a serious limitation for they exhibit unphysical behavior caused by divergences, as we now discuss. In Eqs. (1a)–(1d) level-2.5 models employ the following:

$$\frac{\partial}{\partial t} = 0; \quad \frac{\partial F_w}{\partial z} = 0, \quad \frac{\partial}{\partial z}\overline{w^2\theta} = 0, \quad \frac{\partial}{\partial z}\overline{w\theta^2} = 0. \quad (2a)$$

Thus, the turbulence variables $\overline{w^2}$, $\overline{u^2}$, $\overline{w\theta}$, and $\overline{\theta^2}$ are given by a local model. It is in this sense that we refer to the level-2.5 models as local. The resulting equations become algebraic relations that can be solved analytically. In particular, the vertical heat flux is given by

$$\overline{w\theta} = -K_H\frac{\partial T}{\partial z}, \quad (2b)$$

where K_H is the heat turbulent diffusivity:

$$K_H = K\tau S_H, \quad (2c)$$

where the dimensionless structure function S_H is given by

$$S_H = \frac{2}{3\lambda_5 - (4\lambda_4 + 3\lambda_8)G_h}, \quad G_h = -\tau^2 g\alpha\frac{\partial T}{\partial z}. \quad (2d)$$

Equation (2d) shows that *in unstably stratified flows* $G_h > 0$, S_H diverges for some value of G_h (the λs being positive). In MY82's level-2.5 model, S_H becomes infinity at $G_h(\mathrm{cr}) \sim 8.9$ and thus an artificial limit was imposed on the solutions such that

$$G_h \le G_h(\mathrm{cr}) \sim 8.9. \quad (3a)$$

Due to the difference in modeling the pressure correlations, in the CCH model S_H diverges at a different G_h. Using Table 1 of CCH for the λs yields

$$G_h \le G_h(\mathrm{cr}) \sim 16. \quad (3b)$$

The artificial nature of these limitations can be seen in Fig. 1. Using the large eddy simulation (LES) data of Mironov et al. (2000), in Fig. 1 we plot G_h versus *z/H* (*H* is the PBL height), which exhibits a smooth behavior and no limitation such as in (3a) and (3b) exists; however, both the MY82 model and the CCH model are not realizable for regions of G_h larger than the limits imposed by Eqs. (3a) and (3b), respectively. In summary, while the divergences

$$S_H \to \infty \quad \text{as } G_h \to G_h(\mathrm{cr}) \quad (3c)$$

may be avoided with ad hoc prescriptions such as (3a) and (3b) or with heuristic arguments that limit the value of G_h before it reaches the critical values (e.g., Kantha and Clayson 1994), the root cause of the problem, and thus its possible cure, have not yet been discussed and to do so is the main goal of this paper.

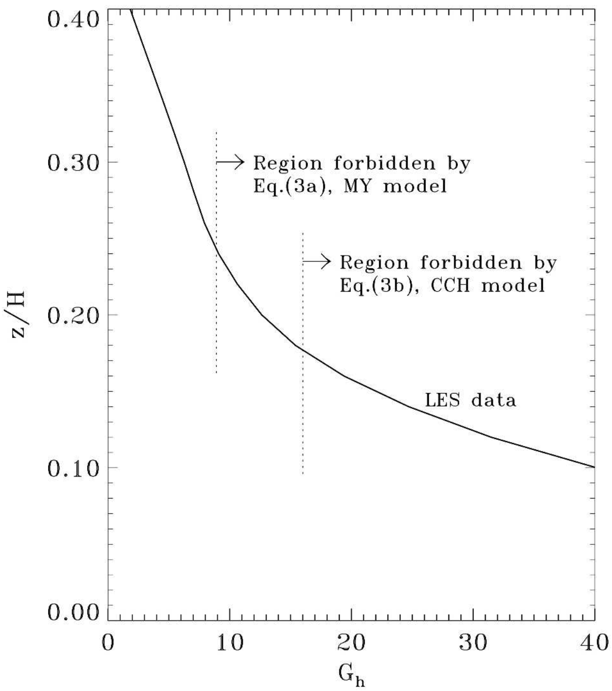

FIG. 1. Both the MY82 model and the CCH model impose limits [Eqs. (3a)–(3b)] to the value of G_h beyond which the models are not realizable. However, the LES data of G_h vs z/H (Mironov et al. 2000, solid line) extend past these limiting values (dotted lines), indicating the deficiencies of the local models.

4. Realizability problem of the local model

Schumann (1977) introduced realizability conditions to be satisfied by turbulence models. As a consequence of Schwarz's inequality, he derived the following conditions:

$$R_{\alpha\beta} \geq 0, \quad \text{for} \quad \alpha = \beta, \tag{4a}$$

$$R_{\alpha\beta}^2 \leq R_{\alpha\alpha} R_{\beta\beta}, \quad \text{for} \quad \alpha \neq \beta, \tag{4b}$$

where $R_{\alpha\beta} = \overline{u_\alpha u_\beta}$ (the Greek indices are not subject to the summation rule). Consider (4a) with $\alpha = \beta = 1, 2$. We have

$$\overline{u^2} \geq 0, \quad \overline{v^2} \geq 0. \tag{4c}$$

Using the level-2.5 model solutions of the RSM equations for a purely convective case [Eqs. (15a) and (15b) in CCH], Eq. (4c) becomes

$$\overline{u^2} = \overline{v^2} = \frac{2}{3} K(1 - \lambda_4 G_h S_H) \geq 0. \tag{4d}$$

An expression analogous to (4d) exists in the MY82 model [their Eqs. (26) and (32b)]. In level-2.5 models, as G_h approaches $G_h(\text{cr})$, $S_H \to \infty$ and the realizability condition (4d) is violated.

5. Nonlocality

The first hint as to the cause of the divergence (3c) comes from considering that it occurs for unstable stratification. Under such conditions, large eddies dominate and their sizes can be of the order of the convective layer itself and yet expressions such as (2b)–(2d) do not exhibit a dependence on H. Relations (2b)–(2d) are local since the heat flux at z depends only on the temperature gradient at the same point. This leads one to conclude that the need for relations such as (3a) and (3b) may be ultimately related to the inability of local expressions such as (2b)–(2d) to fully account for large eddies. As discussed by Stevens (2000), Ertel (1942) was the first to suggest that to account for nonlocality, Eq. (2b) must be modified to

$$\overline{w\theta} = \overline{w\theta}\big|_L + \overline{w\theta}\big|_{\text{NL}}, \tag{4e}$$

where the subscripts L and NL stand for local and nonlocal. The local expression is given by Eqs. (2b)–(2d). In the next section, we derive the nonlocal expression.

6. Nonlocal heat fluxes

In the present study, we will assume that the TOMs are given by LES data and solve (1a)–(1d) for $\overline{w^2}$, $\overline{u^2}$, $\overline{w\theta}$, and $\overline{\theta^2}$ under equilibrium conditions. Instead of (2a) we use

$$\frac{\partial}{\partial t} = 0; \quad \frac{\partial F_w}{\partial z} \neq 0, \quad \frac{\partial}{\partial z}\overline{w^2\theta} \neq 0, \quad \frac{\partial}{\partial z}\overline{w\theta^2} \neq 0. \tag{5a}$$

Equations (1a)–(1d) are now formally solved analytically in terms of the TOMs. The local heat flux is still given by (2b)–(2d):

$$\overline{w\theta}\big|_L = -K\tau S_H \frac{\partial T}{\partial z}, \tag{5b}$$

while the nonlocal part has the following form:

$$\overline{w\theta}\big|_{\text{NL}} = A_1 \frac{\partial \overline{w\theta^2}}{\partial z} + A_2 \frac{\partial \overline{w^2\theta}}{\partial z} + A_3 \frac{\partial F_w}{\partial z}, \tag{5c}$$

where F_w is given by Eq. (1f) and

$$A_1 = -\frac{3}{4}\lambda_8 g\alpha\tau^2 S_H, \quad A_2 = -\frac{3}{2}\tau S_H,$$

$$A_3 = \frac{3}{10}\tau^2 S_H \frac{\partial T}{\partial z}. \tag{5d}$$

Two important features need to be stressed. First, the nonlocal heat flux is represented by the gradient of the third-order moments:

$$\overline{w\theta^2}, \quad \overline{w^2\theta}, \quad \overline{w^3}, \quad \overline{q^2 w}, \quad \overline{pw}, \tag{5e}$$

which are proportional to the flux of temperature variance, the flux of heat flux, the skewness, the flux of turbulent kinetic energy, and the pressure–velocity correlation. Second, each term in (5b) and (5c) is proportional to S_H, which is divergent. However, as we show below, putting together the divergent local and nonlocal terms, the divergences cancel out exactly to yield a finite and smooth total flux.

7. Nonlocal $\overline{u^2}$, $\overline{w^2}$, and $\overline{\theta^2}$

In addition to the nonlocal heat flux, we have also derived the nonlocal expressions for the components of the kinetic energy. The results are

$$\overline{u^2} = \overline{u^2}\Big|_L + \overline{u^2}\Big|_{\mathrm{NL}}, \tag{6a}$$

where

$$\overline{u^2}\Big|_L = \frac{2}{3}K(1 - \lambda_4 G_h S_H), \tag{6b}$$

which is just Eq. (4d). The nonlocal part is given by

$$\overline{u^2}\Big|_{\mathrm{NL}} = B_1\frac{\partial F_w}{\partial z} + B_2\frac{\partial\overline{w^2\theta}}{\partial z} + B_3\frac{\partial\overline{w\theta^2}}{\partial z}, \tag{6c}$$

where [F_w is defined in Eq. (1f)]:

$$B_1 = \frac{1}{20}\tau(1 + 2\lambda_4 G_h S_H), \quad B_2 = \frac{1}{2}\lambda_4 g\alpha\tau^2 S_H,$$

$$B_3 = \frac{1}{2}\lambda_8 g\alpha\tau B_2. \tag{6e}$$

Analogously,

$$\overline{w^2} = \overline{w^2}\Big|_L + \overline{w^2}\Big|_{\mathrm{NL}}, \tag{7a}$$

$$\overline{w^2}\Big|_L = \frac{2}{3}K(1 + 2\lambda_4 G_h S_H), \quad \overline{w^2}\Big|_{\mathrm{NL}} = -2\overline{u^2}\Big|_{\mathrm{NL}}. \tag{7b}$$

Finally, the temperature variance is given by

$$\overline{\theta^2} = \overline{\theta^2}\Big|_L + \overline{\theta^2}\Big|_{\mathrm{NL}}, \tag{8a}$$

where

$$\overline{\theta^2}\Big|_L = \frac{3}{2}\lambda_8 K\tau^2 S_H\left(\frac{\partial T}{\partial z}\right)^2, \tag{8b}$$

$$\overline{\theta^2}\Big|_{\mathrm{NL}} = C_1\frac{\partial\overline{w\theta^2}}{\partial z} + C_2\frac{\partial\overline{w^2\theta}}{\partial z} + C_3\frac{\partial F_w}{\partial z}, \tag{8c}$$

with

$$C_1 = -\frac{3}{4}\lambda_8\tau\left(1 + \frac{3}{2}\lambda_8 G_h S_H\right), \quad C_2 = \frac{9}{4}\lambda_8\tau^2 S_H\frac{\partial T}{\partial z},$$

$$C_3 = -\frac{1}{5}\tau\frac{\partial T}{\partial z}C_2. \tag{8d}$$

As in the case of the nonlocal heat flux, two considerations are in order: all the nonlocal terms are expressed in terms of the TOMs; second, the divergent function S_H is present in all the terms that therefore individually diverge as one approaches G_h(cr). In the next section we show that, in the complete expressions of $\overline{w\theta}$, $\overline{u^2}$, $\overline{w^2}$, and $\overline{\theta^2}$, the divergences cancel out numerically yielding a finite result for all values of G_h.

8. Numerical results

Following a tradition initiated by Moeng and Wyngaard (1986, 1989) and followed by many others (e.g., Holtslag and Moeng 1991; Moeng and Sullivan 1994; Mironov et al. 2000; Nakanishi 2001; Canuto et al. 2001a; Gryanik and Hartmann 2002), we use the LES data to compute the terms in the expressions for $\overline{w\theta}$, $\overline{u^2}$, $\overline{w^2}$, and $\overline{\theta^2}$ presented above. From our experience, to assess a relation among different moments, using the LES data as input is more stringent a test than running a numerical simulation; the former is a direct and straightforward procedure while the latter can be affected by many other factors.

To see more clearly how the divergences cancel out, we rewrite the expression for the complete solution for the heat flux as follows:

$$\overline{w\theta} \equiv \frac{N}{D} = \underbrace{-\frac{2}{D}K\tau\frac{\partial T}{\partial z}}_{\text{Local term}}\ \underbrace{-\frac{3}{2D}\lambda_8 g\alpha\tau^2\frac{\partial\overline{w\theta^2}}{\partial z} - \frac{3\tau}{D}\frac{\partial\overline{w^2\theta}}{\partial z} + \frac{3}{5D}\tau^2\frac{\partial T}{\partial z}\frac{\partial F_w}{\partial z}}_{\text{Nonlocal terms}}, \tag{9a}$$

where

$$N \equiv -2K\tau\frac{\partial T}{\partial z} - \frac{3}{2}\lambda_8 g\alpha\tau^2\frac{\partial\overline{w\theta^2}}{\partial z} - 3\tau\frac{\partial\overline{w^2\theta}}{\partial z} + \frac{3}{5}\tau^2\frac{\partial T}{\partial z}\frac{\partial F_w}{\partial z}, \tag{9b}$$

$$D \equiv 3\lambda_5 - (4\lambda_4 + 3\lambda_8)G_h. \tag{9c}$$

On the right-hand side of (9a), the first term corresponds to the local model, the remaining three terms imply the TOMs, corresponding to the nonlocal terms. This expression comes from combining Eqs. (5b)–(5d). As one can see, the denominator will inevitably vanish at some values of G_h, where the divergence occurs. We found it convenient to adjust the SOC constant λ_8 such that the numerator and the denominator may vanish simultaneously, making it possible for the divergences to cancel out. But this is only a necessary condition to remove the singularity. For the cancellation to really occur in the neighborhood around the zero point of the denominator and yield a smooth, well-behaved $\overline{w\theta}$, the numerator, that is, the TOMs, must be reasonably realistic and well behaved, thus, a good quality TOM model is required. The TOMs obtained from solving the corresponding dynamic equations with QNA for the fourth-order moments (FOMs) do not qualify because the TOM expressions thus obtained diverge themselves.

To be more specific, we use the following procedure to determine λ_8. Using LES data as input, in Fig. 2 we plot the set of values of λ_8 versus G_h that makes D vanish (thick solid line). Similarly, we also plot values of λ_8 that makes N zero (thin solid line). As seen in the figure, the value of λ_8 ($\sim$0.43) is determined as the intersection of these two curves, since it makes both D and N go to zero simultaneously. It is important to stress that for the TOM models of Canuto et al. (1994, 2001a) that are based on the QNA, the above procedure does not work because the TOMs have their own singularities. Therefore, we rely on the LES data for the TOMs. The lesson to be learned is that the QNA-based TOMs, which avoided their own singularities by unrealistically reducing G_h and seem pretty close to the LES values, are actually not sufficiently accurate. Although $\overline{w\theta}$ looks fine, it is at the expense of incorrect G_h, or $T(z)$. In turn, this means QNA is not appropriate. A better model for the fourth-order moments will be needed. One needs both a suitable value of λ_8, which is a second-order closure (SOC) constant, and a high quality non-Gaussian TOM model to solve the singularity problem.

To obtain a complete cancellation of the divergences we employed $\lambda_8 = 0.427$ instead of the CCH value $\lambda_8 = 0.547$. The latter corresponds to the case of isotropic turbulence, whereas the value used here is closer to the value suggested by Shih and Shabbir (1992, their appendix B). To exhibit the cancellation of divergences, in Fig. 3 we plot each term of the total heat flux $\overline{w\theta}$, where curve 1 corresponds to the local term in Eq. (9a), curves 2–4 correspond to the three nonlocal terms in Eq. (9a) in the same order. Due to the zero in D [Eq. (9c)], all of the four terms in $\overline{w\theta}$ diverge at $z/H = 0.16$, and each of them exhibits two discontinuous branches one on each side of the singular point. We also plot curve 5 that represents the total heat flux, local plus nonlocal; the divergences have canceled out entirely. In addition, the

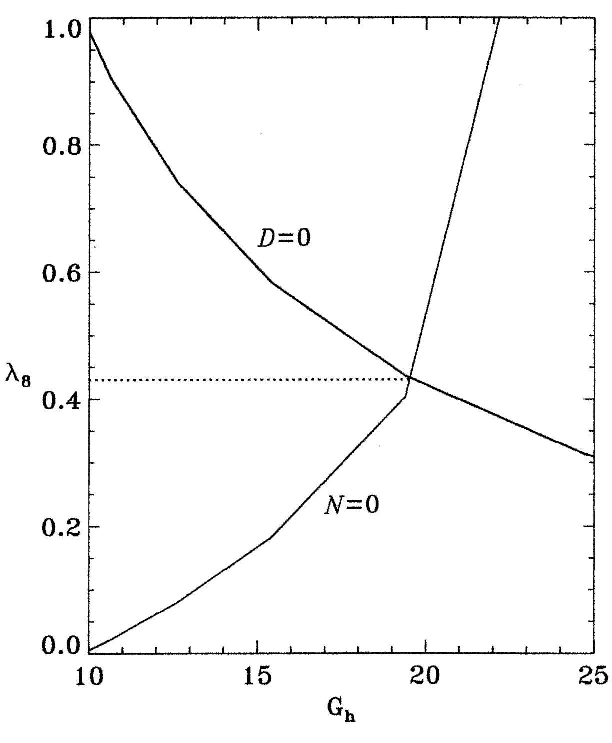

FIG. 2. A procedure is shown to find the suitable value for the SOC constant λ_8. The thick solid line represents the set of possible values of λ_8 that make the denominator of $\overline{w\theta}$ in Eq. (9a) vanish, while the thin solid line represents the set of possible values of λ_8 that make the numerator of $\overline{w\theta}$ vanish. The intersection of these two curves yields the preferred value of λ_8 that makes both the denominator and the numerator vanish simultaneously.

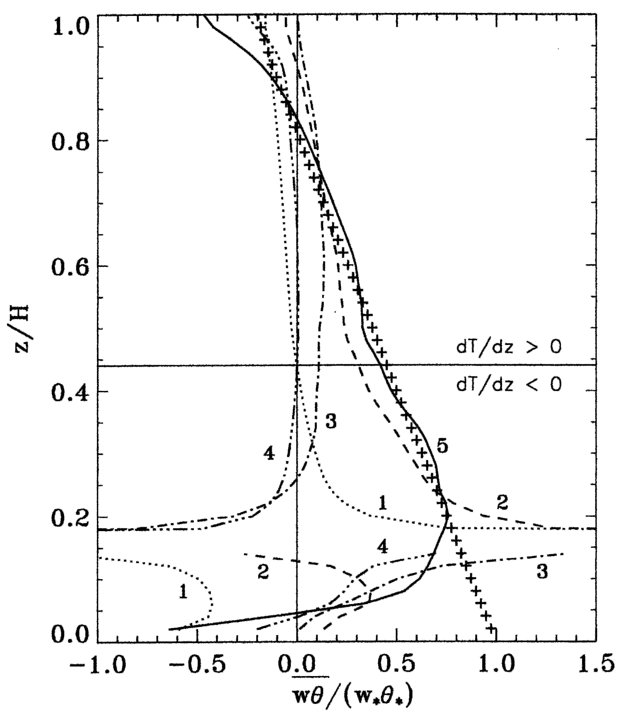

FIG. 3. The total heat flux $\overline{w\theta}$ given by Eq. (9a), normalized by its surface value, vs z/H. In Eq. (9a), the profiles of the turbulent variables $K(z)$, $\tau(z)$, $T(z)$, and TOMs(z) are taken from the LES data of Mironov et al. (2000). Curve 1 represents the local heat flux represented by the first term of Eq. (9a). Curves labeled 2–4 represent the three nonlocal terms [i.e., the second, third, and fourth terms in Eq. (9a)] while curve 5 is the complete expression for the heat flux [i.e., the sum of all four terms]. The divergence of each of the four terms occurs at $z/H = 0.16$, but their sum, curve 5, is finite and smooth. The LES data for $\overline{w\theta}$ are also plotted as crosses.

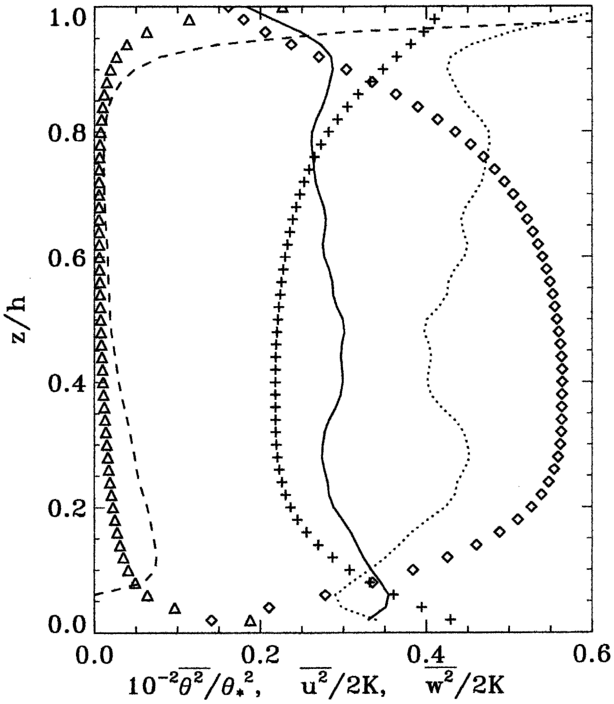

FIG. 4. Plot of normalized $\overline{u^2}/2K$ (solid line), $\overline{w^2}/2K$ (dotted line), and $\overline{\theta^2}$ (dashed line) vs z/H, according to Eqs. (6a)–(8d). The normalized LES data of $\overline{u^2}/2K$ (crosses), $\overline{w^2}/2K$ (diamonds), and $\overline{\theta^2}$ (triangles) of Mironov et al. (2000) are also plotted.

LES data for $\overline{w\theta}$ is plotted as crosses in Fig. 3 for comparison purpose. In Fig. 4 we plot for $\overline{u^2}$, $\overline{w^2}$, and $\overline{\theta^2}$ given by Eqs. (6)–(8) and LES data. The divergence and violation of the realizability condition discussed earlier have all disappeared.

The discrepancies near the surface are explained by Moeng and Sullivan (1994) who pointed out that "the LES results in the surface layer are not reliable since, for typical meshes, simulations cannot resolve small but dominant eddies in the surface layer." Thus, the discrepancies for $z/H < 0.1$ between model results and LES data may not be significant.

Another point to be noticed is that although the above analysis has been carried out in the steady-state limit, it may still be considered as (approximately) valid even when the flow is perturbed somewhat away from the equilibrium conditions, since the unrealistic growth of the second-order moments (SOMs) in the local models occurs not only at a single parameter value but for a range of parameter values, as indicated by Fig. 3.

9. Conclusions

The main goal of this paper was to show that in buoyancy-driven flows, the divergences that characterize the widely used MY-type level-2.5 closure second-order moments do not represent an intrinsic shortcoming of the turbulence model. Rather, they are due to the local approximation. Once the nonlocal terms are properly accounted for, all divergences cancel out and one obtains finite and well-behaved second-order moments in the PBL. This poses the obvious question of how to evaluate the TOMs to represent the nonlocal terms. Since in this paper we were mainly interested in a proof of principle, it was natural to employ LES data for the TOMs. However, using the QNA-based TOMs (e.g., from Canuto et al. 1994, 2001a), the cancellation of divergences does not happen, even if the closure constants are carefully chosen. This indicates that *in order to remove the singularities, one needs both a good SOC model* (obtained here via suitably choosing SOC constants) *and a well-behaved non-Gaussian TOM model.* Constructing the latter is quite a demanding task.

The relations between SOMs and TOMs presented here are derived from the dynamic equations for the SOMs and are quite general. We analyzed these relations and their singularities, and discussed under what conditions the singularities can be removed. We used LES data to show that this is possible. Work is under way to derive a new model for the TOMs, which will be tested under the new, more stringent requirement that they must yield finite second-order moments.

Acknowledgments. We thank Dr. Mironov for providing us the LES data used in our Figs. 1–4.

REFERENCES

Canuto, V. M., 1994: Large eddy simulation of turbulence: A subgrid scale model including shear, vorticity, rotation, and buoyancy. *Astrophys. J.,* **428,** 729–752.

——, F. Minotti, C. Ronchi, R. M. Ypma, and O. Zeman, 1994: Second-order closure PBL model with new third-order moments: Comparison with LES data. *J. Atmos. Sci.,* **51,** 1605–1618.

——, Y. Cheng, and A. Howard, 2001a: New third-order moments for the convective boundary layer. *J. Atmos. Sci.,* **58,** 1169–1172.

——, A. Howard, Y. Cheng, and M. S. Dubovikov, 2001b: Ocean turbulence. Part I: One-point closure model-momentum and heat vertical diffusivities. *J. Phys. Oceanogr.,* **31,** 1413–1426.

Cheng, Y., V. M. Canuto, and A. M. Howard, 2002: An improved model for the turbulent PBL. *J. Atmos. Sci.,* **59,** 1550–1565.

Ertel, H., 1942: Der vertikale Turbulenz-Warmerstrom in der Atmosphere. *Meteor. Z.,* **59,** 250–253.

Gryanik, V. M., and J. Hartmann, 2002: A turbulence closure for the convective boundary layer based on a two-scale mass-flux approach. *J. Atmos. Sci.,* **59,** 2729–2744.

Holtslag, A. A. M., and C.-H. Moeng, 1991: Eddy diffusivity and countergradient transport in the convective atmospheric boundary layer. *J. Atmos. Sci.,* **48,** 1690–1700.

Kantha, L. H., and C. A. Clayson, 1994: An improved mixed layer model for geophysical applications. *J. Geophys. Res.,* **99** (C12), 25 235–25 266.

Mellor, G. L., and T. Yamada, 1974: A hierarchy of turbulence closure models for planetary boundary layer. *J. Atmos. Sci.,* **31,** 1791–1806.

——, and ——, 1982: Development of a turbulence closure model for geophysical fluid problems. *Rev. Geophys. Space Phys.,* **20,** 851–875.

Mironov, D. V., V. M. Gryanik, C.-H. Moeng, D. J. Olbers, and T. H. Warncke, 2000: Vertical turbulence structure and second-moment budgets in convection with rotation: A large-

eddy simulation study. *Quart. J. Roy. Meteor. Soc.,* **126,** 477–515.
Moeng, C. H., and J. C. Wyngaard, 1986: An analysis of closures for pressure-scalar covariances in the convective boundary layer. *J. Atmos. Sci.,* **43,** 2499–2513.
——, and ——, 1989: Evaluation of turbulent transport and dissipation closure in second order modeling. *J. Atmos. Sci.,* **46,** 2311–2330.
——, and P. Sullivan, 1994: A comparison of shear and buoyancy driven planetary boundary layer. *J. Atmos. Sci.,* **51,** 999–1022.
Nakanishi, M., 2001: Improvements of the MY turbulence closure model based on large eddy simulation data. *Bound.-Layer Meteor.,* **99,** 349–378.
Schumann, U., 1977: Realizability of Reynolds stress turbulence models. *Phys. Fluids,* **20,** 721–725.
Shih, T.-H., and A. Shabbir, 1992: Advances in modeling the pressure correlation terms in the second moment equations. *Studies in Turbulence*, T. B. Gatski, S. Sarkar, and C. G. Speziale, Eds., Springer-Verlag, 91–128.
Stevens, B., 2000: Quasi-steady analysis of a PBL model with an eddy-diffusivity profile and non-local fluxes. *Mon. Wea. Rev.,* **128,** 824–836.
Zilitinkevich, S., M. Gryanik, V. N. Lykossov, and D. V. Mironov, 1999: Third-order transport and non-local turbulence closures for convective boundary layers. *J. Atmos. Sci.,* **56,** 3463–3477.